



Article

# Formation of Composite Coatings during Detonation Spraying of $\text{Cr}_3\text{C}_2$

Igor S. Batraev <sup>1</sup>, Vladimir Yu. Ulianitsky <sup>1,2</sup>, Alexandr A. Shtertser <sup>1,\*</sup>, Dina V. Dudina <sup>1,3</sup> and Arina V. Ukhina <sup>3</sup>

<sup>1</sup> Lavrentyev Institute of Hydrodynamics, Siberian Branch of the Russian Academy of Sciences, 630090 Novosibirsk, Russia

<sup>2</sup> Faculty of Aircraft, Novosibirsk State Technical University, 630073 Novosibirsk, Russia

<sup>3</sup> Institute of Solid State Chemistry and Mechanochemistry, Siberian Branch of the Russian Academy of Sciences, 630117 Novosibirsk, Russia

\* Correspondence: asterzer@mail.ru

**Abstract:** In the current practice of applying carbide-based coatings by thermal spraying, the starting material usually contains a metal binder. However, it is important to study the possibility of spraying binder-free carbides, since the metal components usually reduce the operating temperature and corrosion resistance of cermet coatings. In this work, a powder of chromium carbide,  $\text{Cr}_3\text{C}_2$ , was sprayed using a CCDS2000 detonation gun. Acetylene–oxygen mixtures  $\text{C}_2\text{H}_2 + k\text{O}_2$  with  $k$  varying from 0.8 to 3.0 were used as an energetic material. Due to chemical reactions between  $\text{Cr}_3\text{C}_2$  and the detonation products, the coatings were of composite nature (multi-phase materials) with a composition depending on  $k$ . At  $k$  values in the range from 0.8 to 1.1, along with  $\text{Cr}_3\text{C}_2$ , the coatings contained chromium carbonitride  $\text{Cr}_3\text{N}_{0.4}\text{C}_{1.6}$ . In the  $k$  range from 1.3 to 2.0,  $\text{Cr}_7\text{C}_3$  and Cr were the main components of the coatings. As  $k$  was increased to 3.0, along with  $\text{Cr}_7\text{C}_3$  and Cr, the  $\text{CrO}$  and  $\text{Cr}_2\text{O}_3$  oxides formed in the coatings. The mechanical properties and wear resistance of the coatings were found to depend on their phase compositions. Coatings produced by detonation spraying of  $\text{Cr}_3\text{C}_2$  powder may be useful for increasing the corrosion resistance of machine parts to mineral acids and high-temperature oxidation resistance.



**Citation:** Batraev, I.S.; Ulianitsky, V.Y.; Shtertser, A.A.; Dudina, D.V.; Ukhina, A.V. Formation of Composite Coatings during Detonation Spraying of  $\text{Cr}_3\text{C}_2$ . *J. Compos. Sci.* **2023**, *7*, 71. <https://doi.org/10.3390/jcs7020071>

Academic Editor: Francesco Tornabene

Received: 28 December 2022

Revised: 28 January 2023

Accepted: 3 February 2023

Published: 8 February 2023



**Copyright:** © 2023 by the authors. Licensee MDPI, Basel, Switzerland. This article is an open access article distributed under the terms and conditions of the Creative Commons Attribution (CC BY) license (<https://creativecommons.org/licenses/by/4.0/>).

**Keywords:** detonation spraying; acetylene–oxygen mixture; chromium carbide; composite coating; microhardness; bond strength; abrasive wear; residual stresses

## 1. Introduction

Coatings based on chromium carbide with a metal binder (Ni or NiCr) are in high demand in modern industry as protective coatings with good corrosion and abrasive resistance when working in aggressive environments up to a temperature of 900 °C [1]. Such composite coatings, thanks to the metal binder, the content of which is in the range from 10 to 30 wt. %, have good adhesion and cohesion, as well as hardness at the level of 1000 HV<sub>0.3</sub>. Depending on the conditions under which the coating operates, various thermal spray methods can be used: plasma spray (PS) [2,3], high-speed flame spraying using oxygen or air as an oxidizer (HVOF or HVAF) [4,5], detonation spraying [6] and, to a lesser extent, cold spray (CS) [7].

In recent years, there has been increased interest in obtaining ceramic coatings from pure chromium carbide, since such coatings have greater acid resistance compared to composite coatings. For example, in [8],  $\text{Cr}_3\text{C}_2$  coatings were produced by post-treatment of chromium coatings formed by PS and CS methods. Post-treatment was carburization in a methane-containing medium during heat treatment. Thermal reactive diffusion (TRD) is also used to obtain films and thin coatings from pure chromium carbide [9–11]. Finally, in [12], the authors investigated the possibility of spraying a coating of pure chromium carbide by high-velocity suspension flame spraying (HVSFS).

There is no information in the literature on the formation of pure  $\text{Cr}_3\text{C}_2$  coatings by detonation spraying. To fill this gap, this work was aimed at studying the possibility of detonation spraying of pure chromium carbide (without a metal binder) and investigating the composition and properties of the resultant coatings.

## 2. Materials and Methods

In the experiments, a chromium carbide powder ( $\text{Cr}_3\text{C}_2$ ) produced by LLC “Rosnamis” (Taganrog, Russia) was used, which was sieved through a sieve of 20  $\mu\text{m}$ . As shown in Figure 1, the powder particles have an irregular fragmentary shape. According to the microscopic analysis, the bulk of the powder is represented by particles ranging in size from 10  $\mu\text{m}$  to 20  $\mu\text{m}$ .

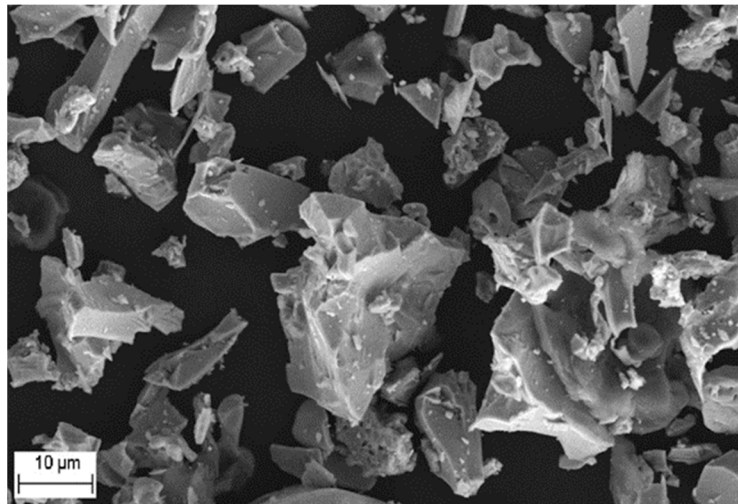


**Figure 1.** Morphology of the  $\text{Cr}_3\text{C}_2$  feedstock powder (Carl Zeiss Merlin electron microscope).

Chromium carbide,  $\text{Cr}_3\text{C}_2$ , is acid-resistant and insoluble in alkaline solutions. These properties make it suitable for applications in the chemical industry.  $\text{Cr}_3\text{C}_2$  has an orthorhombic crystal lattice, a melting point of 2168 K, a modulus of elasticity of 372 GPa, thermal conductivity of  $19.3 \text{ W m}^{-1} \text{ K}^{-1}$ , microhardness of 1040–2020 HV (the spread is associated with the anisotropy of the crystal lattice) and a coefficient of thermal expansion of  $11.7 \times 10^{-6} \text{ K}^{-1}$ . Due to its high melting point, rather high thermal conductivity and high hardness,  $\text{Cr}_3\text{C}_2$  can operate under wear conditions at elevated temperatures in aggressive environments. Since the value of the coefficient of thermal expansion of  $\text{Cr}_3\text{C}_2$  is close to those of steels, it is widely used as a component of coatings with a nickel or nichrome binder. The coatings are deposited by the thermal spray techniques. Unlike WC-based coatings, the cobalt binder is not used in  $\text{Cr}_3\text{C}_2$ -based coatings because of the high solubility of  $\text{Cr}_3\text{C}_2$  in cobalt [12].

Detonation spraying of the chromium carbide powder was carried out using a CCDS2000 detonation gun [13], developed at the Lavrentyev Institute of Hydrodynamics of the Siberian Branch of the Russian Academy of Sciences (LIH SB RAS). Acetylene, oxygen and nitrogen gases of technical purity (impurity concentration < 1%) were used to form an explosive mixture (EM), purge the barrel between the shots (nitrogen) and feed the powder into the gun barrel (nitrogen).

In thermal spray technologies, the coating deposition process is characterized by the deposition efficiency factor (DE), since only a fraction of the particles injected into the barrel of the detonation gun form a coating. Some particles ricochet or splash during the spraying process and are not deposited on the substrate. The DE parameter determines the spraying performance and is one of the optimization criteria of the spraying process. DE was calculated as  $DE = m/m_0$ , where  $m$  is the mass of the material deposited in one shot, and  $m_0$  is the mass of the powder injected into the barrel in one shot.

The morphology of the powder and the microstructure of the coatings were studied by scanning electron microscopy (SEM) on a Carl Zeiss Merlin microscope (Carl Zeiss NTS, Oberkochen, Germany). The X-ray diffraction (XRD) patterns of the initial powder and coatings were recorded using a D8 ADVANCE diffractometer (Bruker AXS, Karlsruhe, Germany) with Cu K $\alpha$  radiation. The optical images were obtained using an OLYMPUS GX-51 metallographic microscope (Tokyo, Japan). The porosity of the coatings was determined by analyzing the optical images of the cross-sections of the samples using OLYMPUS Stream Image Analysis software Stream Essentials 1.9.1 (Tokyo, Japan). The microhardness measurements were carried out using a Vickers DuraScan-50 hardness tester (EMCO-Test, Kuchl, Austria) at a load of 0.1 kg (HV<sub>0.1</sub>) at nine points on the cross-section of the coating. The average microhardness value is presented together with the standard deviation.

During the spraying process, residual stresses may accumulate in the coatings. At a high level of tensile stresses, cracking or peeling of the coating may occur during the spraying process. Therefore, to ensure the reliability and durability of the coating, the formation of moderate residual compression stresses is preferable. The characterization of residual stresses in coatings was carried out by the Almen method [14,15], in which the shape of a standardized steel strip (Almen strip) with a layer of a sprayed coating is analyzed. In the case of tensile stresses in the coating, the Almen strip is bent outward by a steel substrate. In the presence of compressive stresses, the strip is bent outward by the coating. The bond strength of the coatings to the substrate (adhesion) was measured according to the ASTM C633 standard using ULTRABOND-100TM glue. Mechanical tests were carried out on a Zwick Roell Z100 testing machine (ZwickRoell GmbH & Co. KG, Ulm, Germany).

The calculations of the temperature, kinetic head and concentrations of the components of the detonation products (DP) behind a detonation front were carried out using a computer code developed at LIH SB RAS (based on the theoretical model described in [16]). In order to calculate the velocities and temperatures of the sprayed particles, the LIH computer code developed at LIH SB RAS [17] was used. In this code, the dispersion of the molten particles into smaller ones in the barrel of a detonation gun is taken into account. When optimizing the spraying mode, the diameter and length of the gun barrel, the composition and volume of the explosive charge, the place of injection of the powder into the gun barrel and the size of its particles were varied in the calculations.

### 3. Results and Discussion

#### 3.1. Results of Numerical Calculations

As shown in [18,19], an acetylene–oxygen explosive mixture (EM) should be used to implement the detonation spraying of refractory materials (materials with a melting point exceeding 3000 K). Experiments with tungsten carbide, which has a high melting point ( $T_m = 3058$  K), have shown the need to choose the composition of EM in a narrow range, so that the temperature of the detonation products (DP) should be close to the maximum value ( $\approx 4500$  K). The deposition of Cr<sub>3</sub>C<sub>2</sub> ( $T_m = 2168$  K) can presumably be carried out in a wider range of EM compositions, since its melting point is almost 900 K lower. Therefore, the calculations of the main detonation parameters—in particular, the temperature and kinetic head of the DP and their composition—were performed with a variation in the oxygen/carbon ratio  $k$  in the range from 0.8 to 3.0 for the C<sub>2</sub>H<sub>2</sub> +  $k$ O<sub>2</sub> acetylene–oxygen mixtures. The kinetic head is the product of the density and the square of the mass velocity of the DP, divided in half. Note that in fuel-depleted EM ( $k > 1$ ), atomic oxygen is contained in DP, and in fuel-rich EM ( $k < 1$ ), atomic carbon is present in DP. As a result, at high DP temperatures, the presence of atomic oxygen can cause the decarburization of chromium carbide [20], while new carbide phases can form in an environment containing atomic carbon [21].

Figures 2 and 3 show the calculated detonation parameters of acetylene–oxygen C<sub>2</sub>H<sub>2</sub> +  $k$ O<sub>2</sub> mixtures with  $k$  in the range from 0.8 to 3.0. In the entire range  $0.8 \leq k \leq 3.0$ , the temperature of DP does not fall below 4000 K. At  $k = 1.2$ , it reaches a maximum

of 4536 K. This temperature is sufficient for melting refractory materials—for example, metallic tungsten ( $T_m = 3695$  K) or its carbide ( $T_m = 3058$  K). The kinetic head, which determines the acceleration of the particles, remains high (approximately 1.8 MPa) in the  $k$  range from 0.8 to 1.25, with a maximum value of 1.85 MPa reached at  $k = 1$ . Further, with increasing  $k$ , this parameter monotonically decreases and reaches a value of 1.3 MPa at  $k = 3.0$ . Figure 3 shows that in the range  $0.8 \leq k \leq 1.0$ , the main components of DP are reducing agents: CO, H<sub>2</sub> and H. Atomic carbon is also present at a low concentration. At  $k \geq 1.0$ , in the DP, active oxidants, O and OH, appear. Their amounts gradually increase, reaching values of approximately 0.6 mol per mol of C<sub>2</sub>H<sub>2</sub> at  $k = 3.0$ .

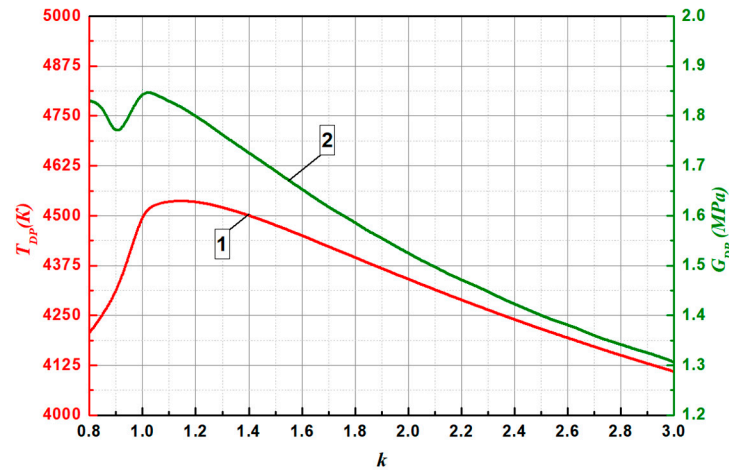


**Figure 2.** The dependence of temperature (curve 1) and kinetic head (curve 2) of DP on the  $k$  parameter of the initial explosive mixture.

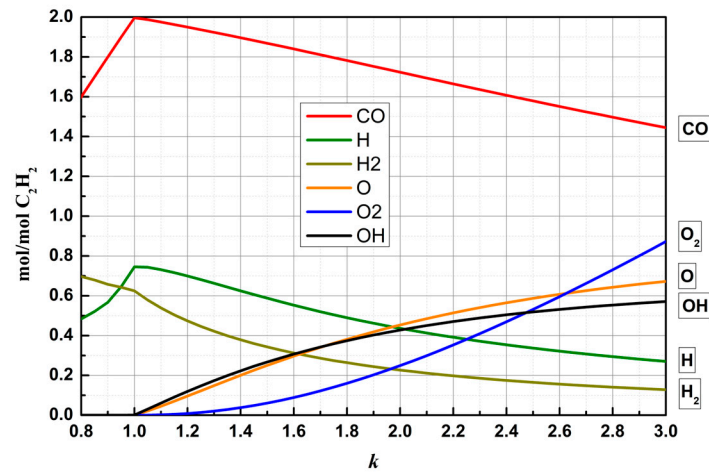
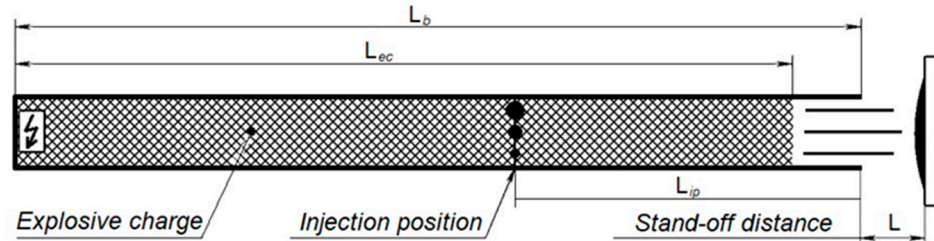


**Figure 3.** The dependence of the content of the main DP components on the  $k$  parameter of the initial explosive mixture.

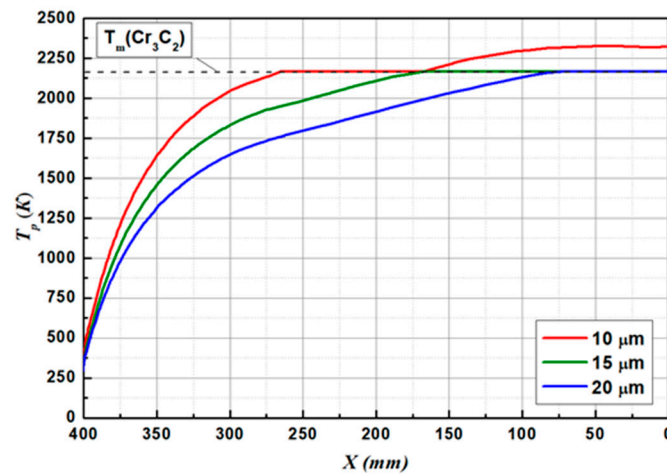
Figure 4 illustrates the detonation spraying process, for which calculations were performed. Calculations for the C<sub>2</sub>H<sub>2</sub> + O<sub>2</sub> ( $k = 1$ ) mixture chosen as the base one showed that, in a barrel with a diameter of 20 mm and a length of 1000 mm, filled with EM up to the powder injection point ( $L_{ip} = L_b - L_{ec}$ ), Cr<sub>3</sub>C<sub>2</sub> particles are heated up to the melting point.

Figure 5 illustrates how the temperature and velocity of the particles change as the latter move from the injection point to the exit from the barrel. As the particle accelerates and moves under the influence of DP, its position in the barrel is described by the  $X$  coordinate, counted from the end of the barrel. It can be seen in Figure 5 that even the largest particles with a size of 20  $\mu\text{m}$  fly out of the barrel in a molten state, when injected at  $L_{ip} = 400$  mm. Particles with a size of 10  $\mu\text{m}$  are heated in the barrel up to the melting point

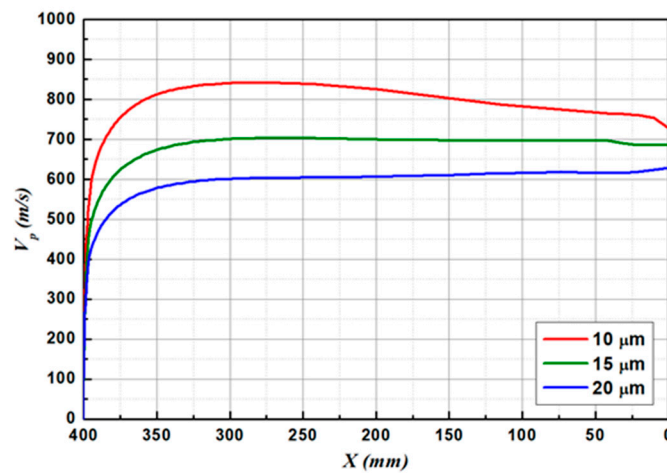
by running 150 mm from the injection point (Figure 5a) and fly out of the barrel in a molten state with a temperature of approximately 2300 K. Other particles with sizes of 15  $\mu\text{m}$  and 20  $\mu\text{m}$  fly out in a molten state with a temperature equal to the melting point. As seen in Figure 5b, the particle velocities at the barrel exit range from 630 m/s to 730 m/s.



**Figure 4.** Detonation spraying scheme:  $L_b$ —barrel length,  $L_{ec}$ —explosive charge length,  $L_{ip}$ —distance from the end of the barrel to the powder injection point,  $L$ —spraying (stand-off) distance.



(a)



(b)

**Figure 5.** Change in temperature (a) and velocity (b) of  $\text{Cr}_3\text{C}_2$  particles as they move from the injection point to the exit from the barrel:  $X$  is the distance from the particle current location to the end of the barrel,  $T_m(\text{Cr}_3\text{C}_2)$  is the melting point of chromium carbide.

Figure 6 shows the evolution of the temperature and velocity of  $\text{Cr}_3\text{C}_2$  particles with a size of 15  $\mu\text{m}$  as the latter move in the barrel for different  $k$  and a constant volume of the explosive mixture. It can be seen that as  $k$  is increased from 1.0 to 2.5, the temperature of the

particles increases to 3000 K (Figure 6a). As  $k$  is further increased, the temperature begins to decrease. The increase in the particle temperature with an increase in  $k$  from 1 to 2.5 is due to an increase in the time of exposure of the particles to hot DP in the detonation gun barrel, since the particle velocity decreases (Figure 6b). The decrease in temperature observed at  $k < 2.5$  is associated with a drop in the DP temperature, the particle velocities remaining sufficiently high. Figure 6 also shows that the value of  $k$  has a much stronger effect on the temperature than on the velocity of the particles flying out of the barrel. The maximum velocity of a particle with a size of 15  $\mu\text{m}$  is gained quickly at a run of approximately 100 mm; at the same time, the temperature at  $k > 1$  is constantly increasing, reaching a maximum at the barrel exit.

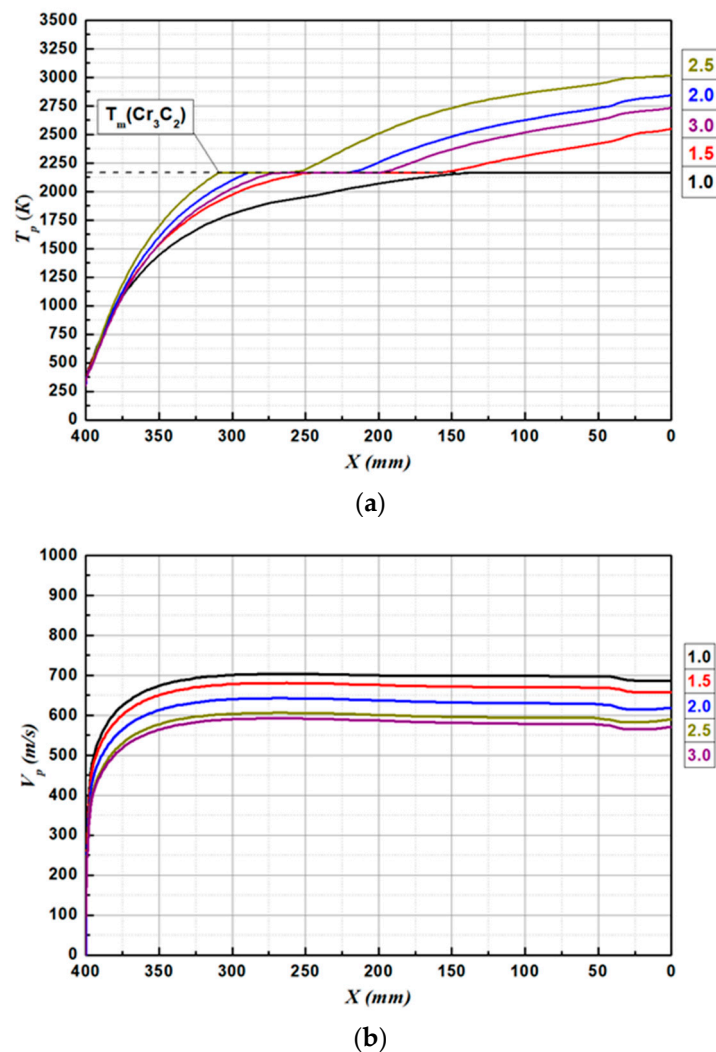


**Figure 6.** The dependence of the temperature (a) and velocity (b) of a  $\text{Cr}_3\text{C}_2$  particle with a size of 15  $\mu\text{m}$  on its position in the barrel for various  $k$  at a constant volume of explosive mixture.

### 3.2. Experimental Results

The experiments on detonation spraying were carried out on a detonation gun with a barrel diameter of 20 mm and a length of 1000 mm. The  $\text{Cr}_3\text{C}_2$  powder was injected into the barrel at a distance of 400 mm from its end. The  $\text{C}_2\text{H}_2 + k\text{O}_2$  explosive mixture filled the barrel up to the injection point of the powder, so that the length of the explosive charge was  $L_{ec} = 600$  mm (see Figure 4). The main goal was to study the effect of  $k$  on the composition and properties of the coatings.

When chromium carbide with a nichrome binder is detonation-sprayed, the spraying distance of  $L = 200 \pm 50$  mm is the optimal one, since, at this spraying distance, the

hardness and wear resistance of the coatings reach their maxima, while the porosity of the coatings does not exceed 0.3% at  $L$  ranging from 50 to 300 mm [6]. Therefore, in this work,  $L = 200$  mm was chosen as the base spraying distance, at which coatings were obtained using different values of  $k$ . The coatings were sprayed onto substrates of low-carbon steel with a size of  $50 \times 70 \times 2$  mm<sup>3</sup>. It was found that the coating was formed only at  $k \geq 0.8$ . An important technological parameter is DE, characterizing the losses of the powder during spraying, as defined in Section 2. At  $k = 0.8$ , up to 40% of the powder is deposited on the substrate, i.e.,  $DE = 40\%$ . Figure 7 illustrates the dependence of DE on  $k$ , showing that in the range of  $k$  from 0.8 to 1.3, the value of DE does not change significantly and is around 40%. With a further increase in  $k$ , DE decreases, remaining at a level of 30% in the  $k$  range of 1.5–3.0.

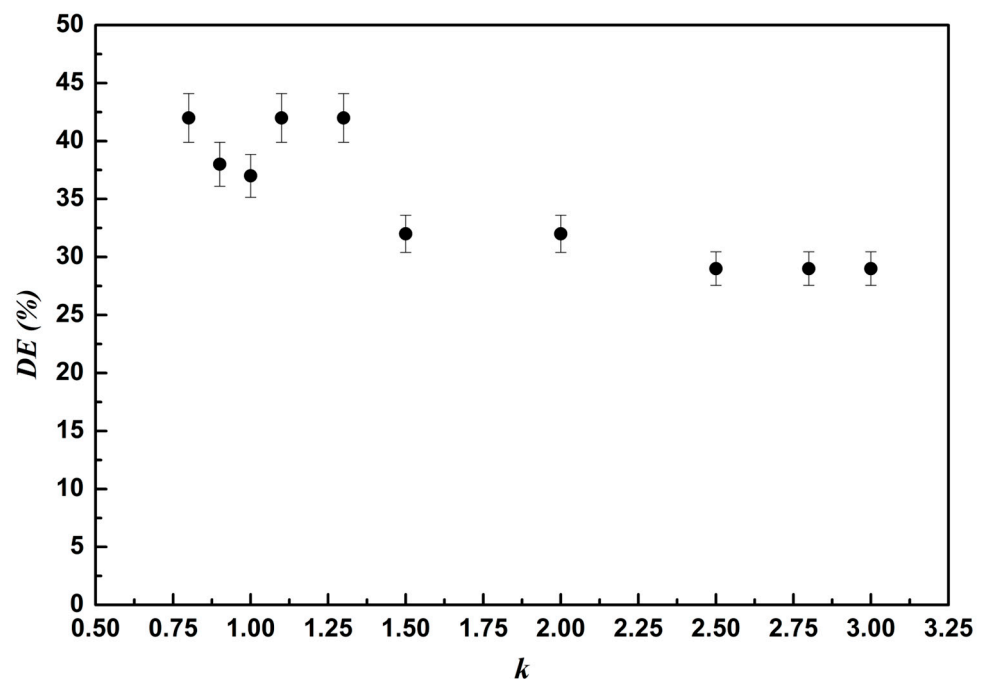


**Figure 7.** The dependence of the deposition efficiency (DE) on  $k$  during detonation spraying of  $\text{Cr}_3\text{C}_2$ .

One of the methods to pre-evaluate the quality of the coating is to study the coating spot formed by a series of shots on a substrate without scanning the surface. Figure 8 shows that, as  $k$  increases from 0.8 to 1.3, the quality of the coating improves, the spot becoming more uniform, showing no traces of erosion of the material. At the same time, the DE remains at a level of 40%. With a further increase in  $k$ , the DE decreases, and, in the range of  $k$  from 1.5 to 3.0, it is at a level of 30% (Figure 7). At  $k$  exceeding 2.0, because of the high concentrations of the oxidizing components in the DP, the decarburization of  $\text{Cr}_3\text{C}_2$  and even the oxidation of metallic chromium occur (Figure 9). As the phase composition of the deposited material changes, the color of the spot also changes, from light gray to dark gray.

Figure 10 shows the microstructure of the coatings obtained at different  $k$ , while Figure 11 shows their hardness and porosity. The coating sprayed at  $k = 0.8$  is characterized by porosity of 2%. With increasing  $k$ , the resultant coatings have a structure consisting of tightly packed lamellae. The porosity of these coatings decreases to 1%.

In accordance with the changes in the phase composition and microstructure, the coatings sprayed at different  $k$  differ in hardness (Figure 11). At  $k = 0.8$  and  $k = 0.9$ , coatings with porosity of 1.5–2.0% and microhardness of approximately 700  $\text{HV}_{0.1}$  are formed. These coatings contain chromium carbide  $\text{Cr}_3\text{C}_2$  and chromium carbonitride  $\text{Cr}_3\text{N}_{0.4}\text{C}_{1.6}$  (Figure 9b). With an increase in  $k$ , the porosity of the coatings drops to 1%: at  $k = 1.0$  and 1.1, the microhardness of the coatings is  $\approx 800$ – $900$   $\text{HV}_{0.1}$ . In the  $k$  range from 1.3 to 2.5, the microhardness drops slightly to  $\approx 700$ – $800$   $\text{HV}_{0.1}$ , apparently due to the presence of

metallic Cr (Figure 9c,d). With a further increase in  $k$  and the formation of oxides in the coatings (Figure 9d), the microhardness increases again.

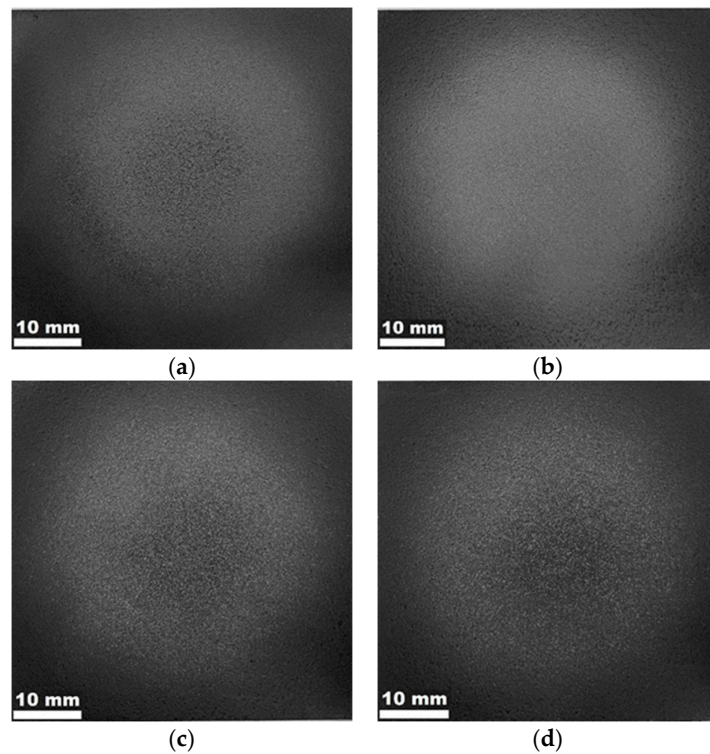


**Figure 8.** Coating spots obtained from the  $\text{Cr}_3\text{C}_2$  powder at different  $k$  values: (a)  $k = 0.8$ , (b)  $k = 1.3$ , (c)  $k = 2.5$ , (d)  $k = 2.8$ .

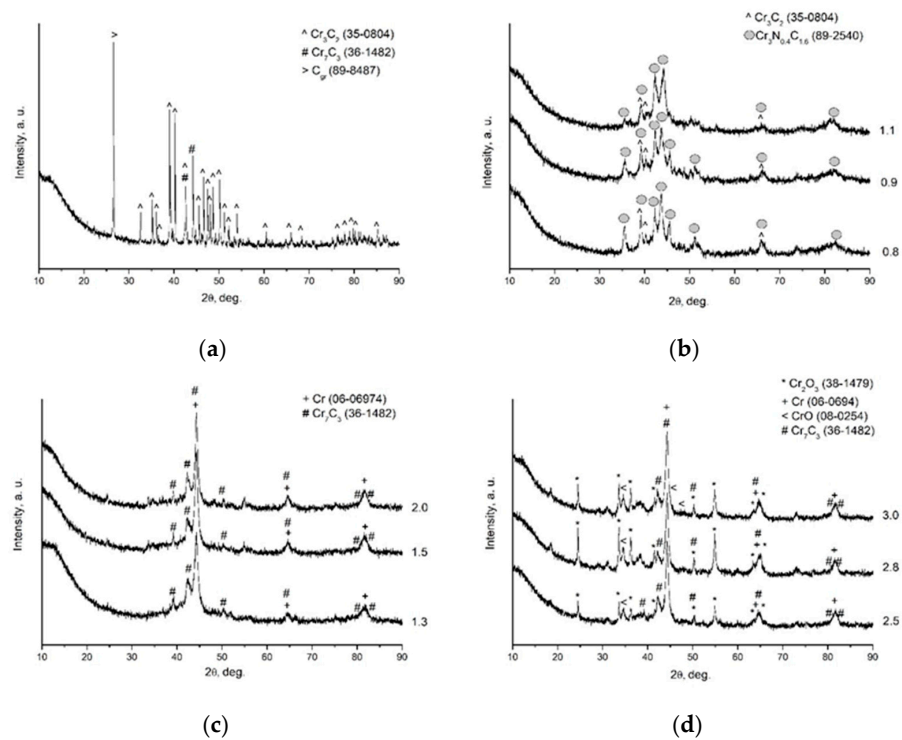


**Figure 9.** XRD patterns of the feedstock powder (a) and coatings obtained at various  $k$ : (b)  $k = 0.8$ , 0.9, 1.1; (c)  $k = 1.3$ , 1.5, 2.0; (d)  $k = 2.5$ , 2.8, 3.0.

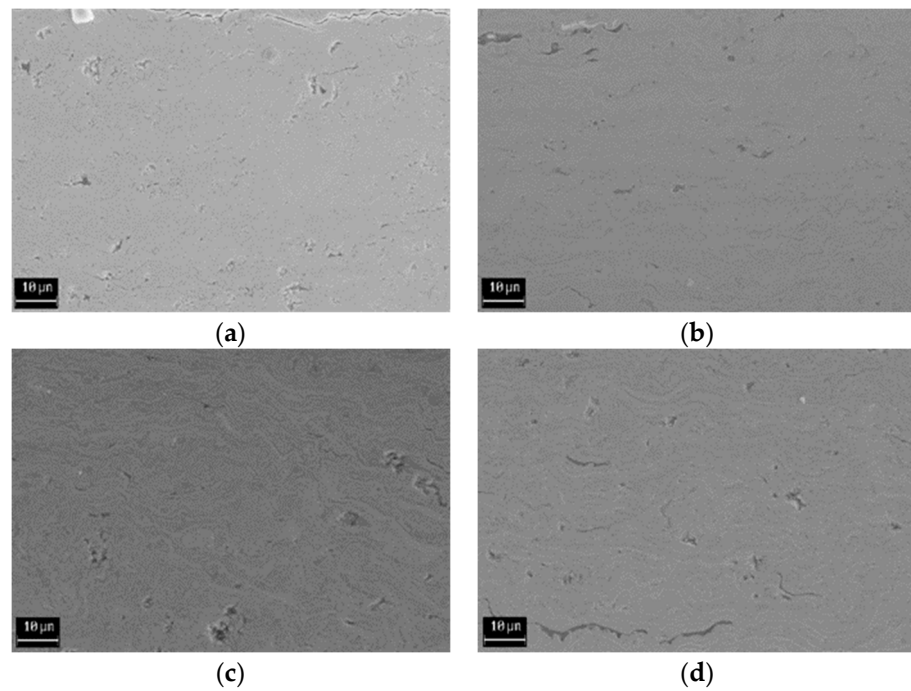


**Figure 10.** Microstructure of the coatings produced from the  $\text{Cr}_3\text{C}_2$  powder at different  $k$ : (a)  $k = 0.8$ , (b)  $k = 1.3$ , (c)  $k = 2.5$ , (d)  $k = 2.8$ .

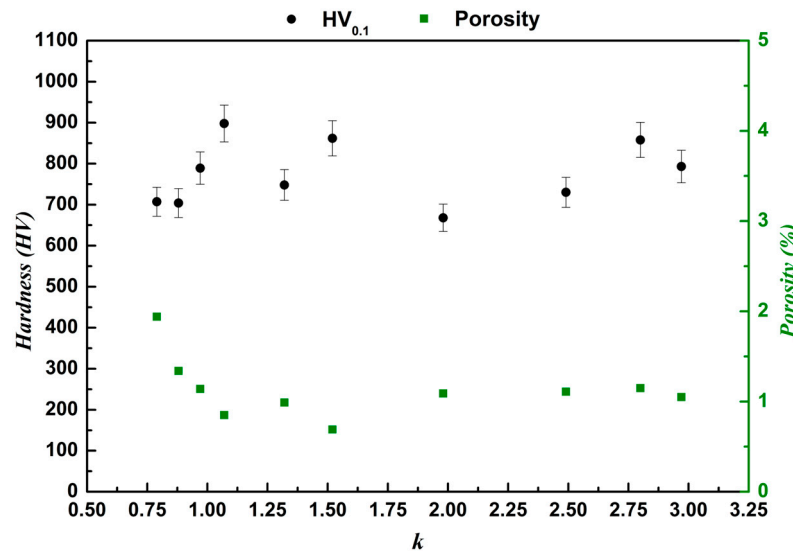


**Figure 11.** The dependence of the microhardness and porosity of the coatings on  $k$ .

The dependence of DE on the spraying distance  $L$  was determined using an explosive mixture with  $k = 1$  (Figure 12). At distances up to 100 mm, DE reaches 50–60%, which is a high value for thermal spraying. As the distance is further increased, the DE monotonously decreases, reaching 25–30% at a distance of 300 mm.

The most important performance characteristics of machine parts with functional coatings, which determine their working life, are the bonding strength of the coating to the substrate (adhesion), the strength of the coating itself (cohesion) and the coating’s resistance to abrasive wear. To study the properties of the coatings, samples were prepared at  $k$  varying from 0.8 to 3.0. The adhesion of the coatings was measured according to the ASTM C633 standard. During testing, the grips of the testing machine clung to the rods, which were glued to the coating and the substrate with ULTRABOND-100TM glue. During testing, the failure of samples occurred through the coating layer, which means that the

coating strength (cohesion) was actually measured. Obviously, in this case, the adhesion was higher than the cohesion. The test results are shown in Figure 13, from which it is clear that the coating strength values are in the range from 19 to 30 MPa.

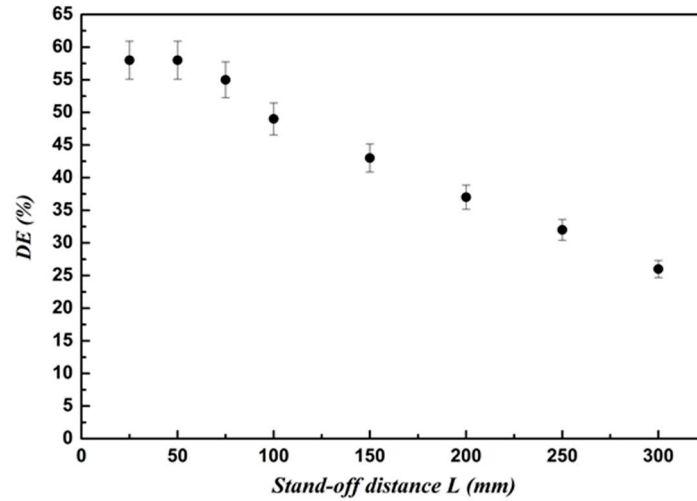


Figure 12. The dependence of the DE on the spraying distance at  $k = 1.0$ .

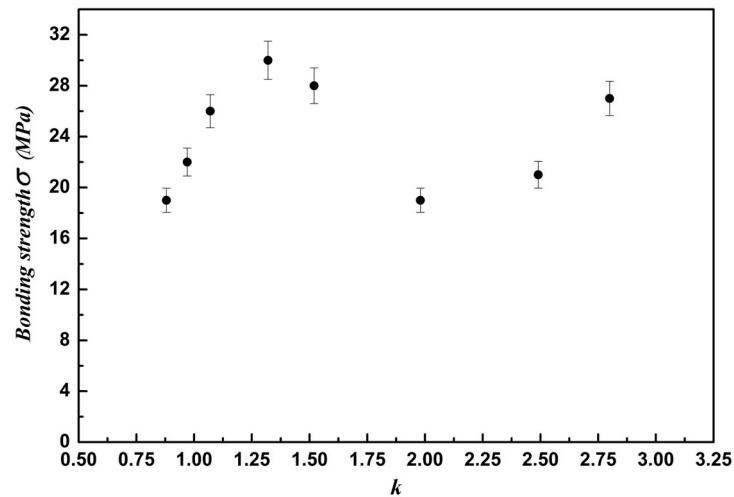


Figure 13. Dependence of the coating strength on  $k$ .

Testing of the coatings under abrasive wear conditions was carried out according to the ASTM G65 standard, according to which the test sample is pressed against a rotating wheel covered with rubber on the rim, and a granular abrasive is fed into the friction zone. The abrasive wear is measured by the loss of sample volume per 1000 revolutions of the rubberized wheel. Before testing, the coatings were ground on a diamond disc. This treatment provides a surface roughness not worse than 0.8 microns, which is required by the ASTM G65 standard. The thickness of the test coatings was  $300 \pm 50$  microns. Testing was performed according to procedure B of the mentioned standard. The sample was pressed against a rubberized disk with a force of 130 N, the total number of revolutions of the disk was 2000 (abrading distance 1436 m), and the consumption of granular abrasive was 300–400 g/min. The dependence of the volumetric wear of the coatings on  $k$  is shown in Figure 14.

As seen in Figure 14, coatings sprayed at  $k = 0.8$  and  $k = 0.9$  are characterized by the maximum wear. This can be explained by the low microhardness, low cohesion and high porosity of these coatings (Figures 11 and 13). With increasing  $k$ , coatings consisting of chromium carbide  $\text{Cr}_3\text{C}_2$  and chromium carbonitride  $\text{Cr}_3\text{N}_{0.4}\text{C}_{1.6}$  become denser and

have higher microhardness and cohesion, which leads to a decrease in wear to a level of  $15 \text{ mm}^3/1000 \text{ rev}$ . In the range of  $k$  from 1.3 to 2.0, dense, but less hard coatings are obtained due to the formation of metallic chromium (Figure 9c). As a result, their wear increases to  $20 \text{ mm}^3/1000 \text{ rev}$ . Chromium oxides are formed in coatings sprayed with near-stoichiometric compositions of the acetylene–oxygen explosive mixture ( $k = 2.0\text{--}3.0$ ), which again leads to an increase in the resistance of the coatings to abrasive wear, which decreases to  $15 \text{ mm}^3/1000 \text{ rev}$ .

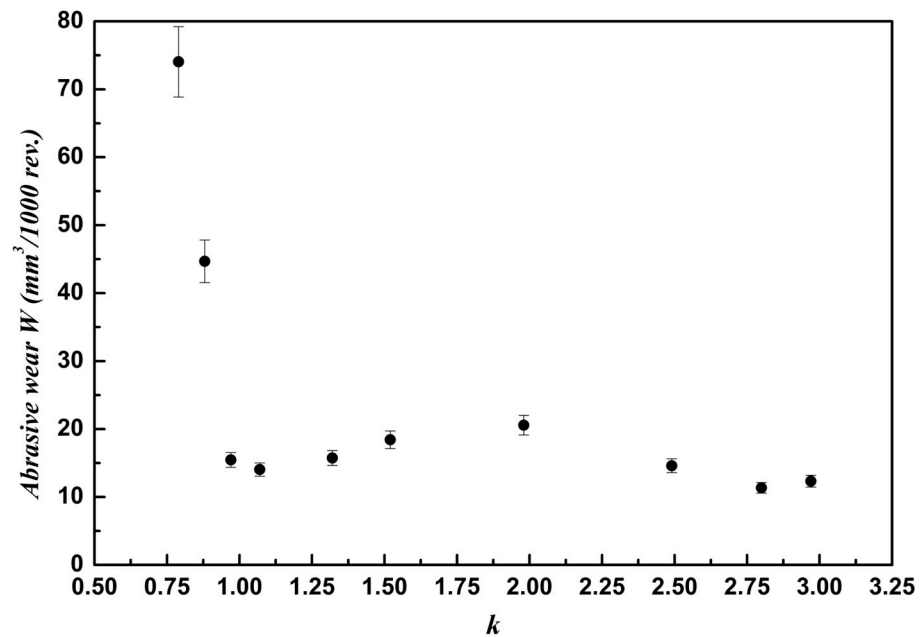


Figure 14. The dependence of abrasive wear on the  $k$  parameter.

To assess the residual stresses in the coatings, tests were carried out using the Almen method [14,15]. According to this method, residual stresses in the coating are calculated from the measured deflection of a thin metal substrate (strip), on which the coating is applied. In our experiments, a coating with a thickness of  $100 \pm 20 \mu\text{m}$  was applied to an Almen strip of type N grade 1 with a size of  $75 \times 19 \times 0.8 \text{ mm}^3$ , manufactured by Electronics Inc. (Mishawaka, IN, USA). After spraying, the strip bent under the influence of internal stresses so that the coating was on its convex surface (Figure 15). This type of deflection corresponds to compressive residual stresses in the coating. The deflection of the Almen strip with the applied coating was  $720 \mu\text{m}$ .



Figure 15. Almen strip with a composite coating produced by spraying the  $\text{Cu}_3\text{C}_2$  powder at  $k = 1.1$ .

The average level of residual stresses in the coating was estimated using the following formula [15]:

$$\sigma_r = \frac{4E\delta^2h}{3t(1-\mu)(4h^2 + l^2)} \quad (1)$$

where  $E$ ,  $\mu$ ,  $\delta$  and  $l$  are the Young's modulus, Poisson's ratio and the thickness and length of the Almen strip;  $t$  is the thickness of the coating, and  $h$  is the deflection of the Almen

strip. For an Almen strip made of SAE 1070 steel,  $E = 2 \cdot 10^5$  MPa,  $\mu = 0.3$ ,  $\delta = 0.8$  mm,  $l = 75$  mm. With a coating thickness of  $t = 0.1$  mm and a deflection of the Almen strip of  $h = 0.72$  mm, the calculation according to (1) gives the value of compressive residual stresses of  $\sigma_r = 312$  MPa.

In the detonation spraying practice, it is known that an increase in the thickness of the coatings can sometimes lead to the formation of cracks and even the detachment of the coating from the substrate. However, in the present work, in the coatings up to 500  $\mu\text{m}$  thick, sprayed on substrates of low-carbon steel with a size of  $70 \times 70$  mm<sup>2</sup>, no signs of peeling or cracking were found.

### 3.3. Discussion

This work demonstrated the possibility of the detonation spraying of a binder-free  $\text{Cr}_3\text{C}_2$  powder for the first time. Chromium carbide has a high melting point; therefore, high-energy acetylene–oxygen detonating mixtures ( $\text{C}_2\text{H}_2 + k\text{O}_2$ ) were chosen for the spraying. The  $k$  parameter reflects the oxygen to carbon molar ratio in the mixture. The calculation of the temperature and kinetic head of the detonation products, as well as the temperatures and velocities of the powder particles accelerated in the barrel of the detonation gun, proved the possibility of forming coatings from a  $\text{Cr}_3\text{C}_2$  powder in a wide range of compositions of acetylene–oxygen explosive mixtures, with  $k$  varying between 0.8 and 3.0.

The experiments described above have shown that the phase and chemical composition of the coatings produced by the detonation spraying of a  $\text{Cr}_3\text{C}_2$  powder change with  $k$  (Figure 9). Due to the chemical interactions of the powder particles with the active components of the DPs in the barrel of the detonation gun, composite coatings are formed. In particular, at  $k$  ranging from 0.8 to 1.1, along with  $\text{Cr}_3\text{C}_2$ , the coatings contain chromium carbonitride,  $\text{Cr}_3\text{N}_{0.4}\text{C}_{1.6}$ . At  $k$  ranging from 1.3 to 2.0, the main phases in coatings are  $\text{Cr}_7\text{C}_3$  and Cr. In the coatings obtained at higher  $k$ , CrO and  $\text{Cr}_2\text{O}_3$  are present, along with the carbide phase,  $\text{Cr}_7\text{C}_3$ , and metallic chromium. Thus, ceramic coatings are formed only at values of  $k$  up to 1.1. At  $k$  exceeding 1.1, cermet coatings are formed. This is due to the appearance of oxidizing components (O,  $\text{O}_2$ , OH) in the detonation products (Figure 3), which leads to the decarburization of  $\text{Cr}_3\text{C}_2$ .

Due to the high particle velocity and, accordingly, the manifestation of the peening effect, coatings with compressive residual stresses are formed. This is important from the point of view of the practical use of these coatings, since the compressive residual stresses are known to increase the fatigue strength of materials. The strength tests of the coatings by the glue method have shown that the bond strength of the coatings to the steel substrate (adhesion) is higher than the strength of the coating itself (cohesion), the latter reaching 30 MPa.

Interestingly, the resistance of the coatings to abrasive wear was found to be very sensitive to parameter  $k$  of the detonating mixture. Namely, in the range of  $k$  from 0.8 to 1.1, the wear resistance increases almost five-fold, and, with a further increase in  $k$ , it does not change significantly. Such an increase in the wear resistance seems to be associated with the transition from a ceramic to a cermet coating.

It should be noted that the mechanical properties and abrasive wear resistance of the coatings elaborated in the present study are inferior to those of  $\text{Cr}_3\text{C}_2$ -based detonation coatings with a nichrome binder [6]. A coating with 20 wt. % of nichrome binder has microhardness of 1150  $\text{HV}_{0.3}$ , strength of at least 150 MPa and abrasive wear of 3.25 mm<sup>3</sup>/1000 rev. However, nichrome melts at 1373 K (solidus temperature). It can be assumed that coatings made by spraying binder-free  $\text{Cr}_3\text{C}_2$  will be able to withstand higher temperatures. Note that metallic chromium is a refractory metal and has a melting point of 2073 K. Thus, all components of the composite coatings produced by spraying  $\text{Cr}_3\text{C}_2$  are refractory.

In addition to corrosion-resistant ceramic, cermet and metallic materials, corrosion-resistant polymers have been developed [22]. Polymer materials are promising for a broad range of applications as the properties of the polymer matrices can be significantly im-

proved by the modifying additives [23–26]. As emphasized in [23], such materials “have high fracture toughness, light weight, superior strength to weight ratio, high tensile properties, high fatigue resistance, and improved corrosion resistance to severe environments”. However, polymers have much lower melting and decomposition temperatures and cannot compete with chromium carbide coatings operating at high temperatures.

Thus, the conducted research has shown that, by the detonation spraying of a  $\text{Cr}_3\text{C}_2$  powder, it is possible to develop composite coatings, the phase and elemental composition of which differ significantly from the initial composition of the feedstock powder. Coatings produced by the detonation spraying of  $\text{Cr}_3\text{C}_2$  powders may be useful for increasing the corrosion resistance of machine parts to mineral acids and high-temperature oxidation resistance. Further studies should focus on evaluating the coating performance under these conditions.

#### 4. Conclusions

The possibility of applying chromium carbide coatings without a metal binder by detonation spraying has been proven. The conducted studies have shown that

- for producing the coatings, acetylene–oxygen mixtures of  $\text{C}_2\text{H}_2 + k\text{O}_2$  with  $k$  values in the range from 0.8 to 3.0 can be used as an explosive;
- due to the chemical interactions of the detonation products with the powder, spraying of  $\text{Cr}_3\text{C}_2$  leads to the formation of composite coatings of various compositions, depending on  $k$ ;
- in the range  $k$  from 0.8 to 1.1, ceramic coatings containing  $\text{Cr}_3\text{C}_2$  and  $\text{Cr}_3\text{N}_{0.4}\text{C}_{1.6}$  carbonitride form; when  $k$  varies from 1.1 to 3.0, the coatings are cermets containing  $\text{Cr}_7\text{C}_3$  and Cr; herewith, at  $k$  greater than 2.0, CrO and  $\text{Cr}_2\text{O}_3$  oxides appear in the coatings;
- the lowest wear resistance (abrasive wear  $W = 74 \text{ mm}^3/1000 \text{ rev.}$ ) was observed in coatings produced at  $k = 0.8$ , when the cohesion ( $\sigma = 19 \text{ MPa}$ ) and microhardness ( $700 \text{ HV}_{0.1}$ ) were also at their minimal levels;
- the maximum wear resistance (abrasive wear  $W = 15 \text{ mm}^3/1000 \text{ rev.}$ ) was observed in coatings obtained at  $k > 1$ ; in this case, the cohesion is maximum ( $\sigma = 26\text{--}30 \text{ MPa}$ ) when  $k = 1.1\text{--}1.4$ , and the microhardness is maximum ( $900 \text{ HV}_{0.1}$ ) when  $k = 1.1$ .

From the point of view of the wear resistance, cohesion and hardness of the coatings, detonation spraying at  $k = 1.1\text{--}1.4$  can be recommended as the optimal mode. However, if, for some reason, the presence of chromium oxides is necessary in the composition of a cermet coating, spraying at  $k$  values close to 3.0 is preferable.

**Author Contributions:** Conceptualization, I.S.B. and V.Y.U.; methodology, V.Y.U. and A.A.S.; software, I.S.B.; investigation, D.V.D., A.V.U. and I.S.B.; writing—original draft, A.A.S.; writing—review and editing, D.V.D., I.S.B. and V.Y.U. All authors have read and agreed to the published version of the manuscript.

**Funding:** This research received no external funding.

**Data Availability Statement:** Not applicable.

**Conflicts of Interest:** The authors declare no conflict of interest.

#### References

1. Berger, L.-M. Application of Hardmetals as Thermal Spray Coatings. *Int. J. Refract. Met. Hard Mater.* **2015**, *49*, 350–364.
2. Li, J.; Zhang, Y.; Huang, J.; Ding, C. Mechanical and Tribological Properties of Plasma-Sprayed  $\text{Cr}_3\text{C}_2\text{-NiCr}$ , WC-Co, and  $\text{Cr}_2\text{O}_3$  Coatings. *J. Therm. Spray Technol.* **1998**, *7*, 242–246.
3. Dzhurinskiy, D.; Babu, A.; Pathak, P.; Elkin, A.; Dautov, S.; Shornikov, P. Microstructure and wear properties of atmospheric plasma-sprayed  $\text{Cr}_3\text{C}_2\text{-NiCr}$  composite coatings. *Surf. Coat. Technol.* **2021**, *428*, 127904. [[CrossRef](#)]
4. Janka, L.; Norpoth, J.; Trache, R.; Berger, L.-M. Influence of Heat Treatment on the Abrasive Wear Resistance of a  $\text{Cr}_3\text{C}_2\text{-NiCr}$  Coating Deposited by an Ethene-Fuelled HVOF Spray Process. *Surf. Coat. Technol.* **2016**, *291*, 444–451. [[CrossRef](#)]
5. Alroy, R.J.; Kamaraj, M.; Sivakumar, G. HVOF vs oxygenated HVOF spraying: Fundamental understanding to optimize  $\text{Cr}_3\text{C}_2\text{-NiCr}$  coatings for elevated temperature erosion resistant applications. *J. Mater. Process. Technol.* **2022**, *309*, 117735.

6. Ulianitsky, V.Y.; Batraev, I.S.; Rybin, D.K.; Dudina, D.V.; Shtertser, A.A.; Ukhina, A.V. Detonation Spraying of Cr<sub>3</sub>C<sub>2</sub>-NiCr Coatings and Their Properties. *J. Therm. Spray Technol.* **2022**, *31*, 598–608. [[CrossRef](#)]
7. Singh, H.; Sidhu, T.S.; Karthikeyan, J.; Kalsi, S.B.S. Development and Characterization of Cr<sub>3</sub>C<sub>2</sub>-NiCr Coated Superalloy by Novel Cold Spray Process. *Mater. Manuf. Process.* **2016**, *31*, 1476–1482.
8. Brupbacher, M.C.; Zhang, D.; Buchta, W.M.; Graybeal, M.L.; Rhim, Y.-R.; Nagle, D.C.; Spicer, J.B. Synthesis and characterization of binder-free Cr<sub>3</sub>C<sub>2</sub> coatings on nickel-based alloys for molten fluoride salt corrosion resistance. *J. Nucl. Mater.* **2015**, *461*, 215–220.
9. Su, X.; Zhao, S.; Sun, H.; Yang, X.; Zhang, P.; Xie, L. Chromium carbide coatings produced on ductile cast iron QT600-3 by thermal reactive diffusion in fluoride salt bath: Growth behavior, microstructure evolution and kinetics. *Ceram. Int.* **2019**, *45*, 1196–1201.
10. Ganji, O.; Sajjadi, S.A.; Yang, Z.G.; Mirjalili, M.; Najari, M.R. On the formation and properties of chromium carbide and vanadium carbide coatings produced on W1 tool steel through thermal reactive diffusion (TRD). *Ceram. Int.* **2020**, *46*, 25320–25329. [[CrossRef](#)]
11. Ganji, O.; Sajjadi, S.A.; Yang, Z.G.; Mirjalili, M. Tribological properties of duplex coatings of chromium-vanadium carbide produced by thermo-reactive diffusion (TRD). *Ceram. Int.* **2022**, *48*, 7475–7490. [[CrossRef](#)]
12. Förg, A.; Blum, M.; Killinger, A.; Nicolás, J.A.M.; Gadow, R. Deposition of chromium oxide-chromium carbide coatings via high velocity suspension flame spraying (HVSFS). *Surf. Coat. Technol.* **2018**, *351*, 171–176.
13. Ulianitsky, V.; Shtertser, A.; Zlobin, S.; Smurov, I. Computer-Controlled Detonation Spraying: From Process Fundamentals Toward Advanced Applications. *J. Therm. Spray Technol.* **2011**, *20*, 791–801. [[CrossRef](#)]
14. Guagliano, M. Relating Almen intensity to residual stresses induced by shot peening: A numerical approach. *J. Mater. Process. Technol.* **2001**, *110*, 277–286. [[CrossRef](#)]
15. Tillmann, W.; Hagen, L.; Luo, W. Process Parameter Settings and Their Effect on Residual Stresses in WC/W<sub>2</sub>C Reinforced Iron-Based Arc Sprayed Coatings. *Coatings* **2017**, *7*, 125.
16. Prueel, E.; Vasil'ev, A. Equation of State of Gas Detonation Products. Allowance for the Formation of the Condensed Phase of Carbon. *Combust. Explos. Shock Waves* **2021**, *57*, 576–587.
17. Gavrilenko, T.P.; Nikolaev, Y.A.; Ulianitsky, V.Y.; Kim, M.C.; Hong, J.W. Computational Code for Detonation Spraying Process. In *Proceedings of the Thermal Spray: Meeting the Challenges of the 21st Century, Nice, France, 25–29 May 1998*; Coddet, C., Ed.; ASM International: Materials Park, OH, USA, 1998; pp. 1475–1483.
18. Ulianitsky, V.; Batraev, I.; Shtertser, A.; Dudina, D.; Bulina, N.; Smurov, I. Detonation spraying behaviour of refractory metals: Case studies for Mo and Ta-based powders. *Adv. Powder Technol.* **2018**, *29*, 1859–1864. [[CrossRef](#)]
19. Rybin, D.; Batraev, I.; Dudina, D.; Ukhina, A.; Ulianitsky, V. Deposition of tungsten coatings by detonation spraying. *Surf. Coat. Technol.* **2021**, *409*, 126943.
20. Babu, P.; Basu, B.; Sundararajan, G. Processing–structure–property correlation and decarburization phenomenon in detonation sprayed WC–12Co coatings. *Acta Mater.* **2008**, *56*, 5012–5026.
21. Ulianitsky, V.Y.; Dudina, D.V.; Batraev, I.S.; Kovalenko, A.I.; Bulina, N.V.; Bokhonov, B.B. Detonation spraying of titanium and formation of coatings with spraying atmosphere-dependent phase composition. *Surf. Coat. Technol.* **2015**, *261*, 174–180.
22. Fuseini, M.; Zaghoul, M.M.Y. Investigation of Electrophoretic Deposition of PANI Nano fibers as a Manufacturing Technology for corrosion protection. *Prog. Org. Coat.* **2022**, *171*, 107015. [[CrossRef](#)]
23. Zaghoul, M.Y.M.; Zaghoul, M.M.Y.; Zaghoul, M.M.Y. Developments in polyester composite materials—An in-depth review on natural fibres and nano fillers. *Compos. Struct.* **2021**, *278*, 114698. [[CrossRef](#)]
24. Mahmoud Zaghoul, M.Y.; Yousry Zaghoul, M.M.; Yousry Zaghoul, M.M. Physical analysis and statistical investigation of tensile and fatigue behaviors of glass fiber-reinforced polyester via novel fibers arrangement. *J. Compos. Mater.* **2023**, *57*, 147–166. [[CrossRef](#)]
25. Zaghoul, M.M.Y.; Steel, K.; Veidt, M.; Heitzmann, M.T. Wear behaviour of polymeric materials reinforced with man-made fibres: A comprehensive review about fibre volume fraction influence on wear performance. *J. Reinf. Plast. Compos.* **2022**, *41*, 215–241.
26. Zaghoul, M.M.Y.; Zaghoul, M.Y.M.; Zaghoul, M.M.Y. Experimental and modeling analysis of mechanical-electrical behaviors of polypropylene composites filled with graphite and MWCNT fillers. *Polym. Test.* **2017**, *63*, 467–474.

**Disclaimer/Publisher's Note:** The statements, opinions and data contained in all publications are solely those of the individual author(s) and contributor(s) and not of MDPI and/or the editor(s). MDPI and/or the editor(s) disclaim responsibility for any injury to people or property resulting from any ideas, methods, instructions or products referred to in the content.